

# The influence of leaf anatomical traits on photosynthesis in Catimor type Arabica coffee

Ziwei Xiao<sup>#\*</sup>, Guanrun Ma<sup>#\*</sup>, Xuehui Bai, Jinhong Li, Mingzhu Zhao, Linlin Su and Hua Zhou

Dehong Tropical Agriculture Research Institute of Yunnan, Ruili 678600, Yunnan, China

<sup>#</sup> These authors contributed equally: Ziwei Xiao, Guanrun Ma

\* Corresponding authors, E-mail: [xiaozw86@126.com](mailto:xiaozw86@126.com); [marui1956@126.com](mailto:marui1956@126.com)

## Abstract

Leaf photosynthesis is largely determined by anatomical features. This study aimed to reveal the quantitative effects of the anatomical structure of *Coffea arabica* leaves on photosynthesis. Pearson's correlation and path analysis were used to explore the correlation between leaf structure and photosynthesis. To calculate the comprehensive evaluation value of the correlation between leaf anatomical traits and photosynthetic parameters, the Criteria Importance Through Intercriteria Correlation (CRITIC) method was used to obtain the objective weight of each photosynthetic parameter. The study revealed that leaf anatomical traits were highly significant ( $p < 0.01$ ) and correlated with photosynthetic parameters, suggesting that anatomical traits greatly influenced photosynthesis in *C. arabica* leaf. Similarly, path coefficient analysis strongly showed direct and indirect correlation of photosynthetic capacity of stomatal conductance of the leaves of *C. arabica*. The results of the comprehensive evaluation also indicated that leaf thickness (LT) and stomatal density ( $d$ ) were the anatomical characteristics most closely related to photosynthesis. In these results, understanding the effects of the anatomical structure of coffee leaves on photosynthesis, may provide useful information for coffee breeding programs and the management of coffee plantations to optimize photosynthetic capacity.

**Citation:** Xiao Z, Ma G, Bai X, Li J, Zhao M, et al. 2024. The influence of leaf anatomical traits on photosynthesis in Catimor type Arabica coffee. *Beverage Plant Research* 4: e002 <https://doi.org/10.48130/bpr-0023-0035>

## Introduction

Coffee (*Coffea arabica*) considered an important tropical crop, is one of the most traded agricultural products in the world. Under suboptimal growing conditions, shade trees, which could reduce the stress on coffee by ameliorating adverse climatic conditions, have been recommended<sup>[1,2]</sup>. Yunnan province, located in Southwest China, is the most suitable region for coffee production in China<sup>[3]</sup>. Although the mountainous landscape and mild climate in this region are well-suited to coffee production, many areas are suboptimal for coffee cultivation<sup>[3,4]</sup>. Thus, agroforestry systems have been recommended for these areas, especially at altitudes below 1,000 m<sup>[4]</sup>.

Since leaves are specialized organs that are responsible for interception of light and uptake of CO<sub>2</sub> through the stomata for photosynthesis<sup>[5]</sup>, light and CO<sub>2</sub> availability in the mesophyll of plant leaves largely determine the net carbon assimilation rate (A) of leaves<sup>[1]</sup>. To analyze the response of photosynthesis to irradiance, the light response curves (LRCs) were used to describe the relationship between photosynthesis and light intensity<sup>[6]</sup>. It is an important method to elucidate the response mechanism of photosynthesis and evaluate photosynthetic efficiency by fitting of light-response model<sup>[5]</sup>. Often, LRCs are mathematically described using empirical models. The light response curves (LRCs) can be used to derive key photosynthetic parameters including the maximum net photosynthetic capacity ( $P_{max}$ ), initial and apparent quantum yields (IQY and AQY), light compensation point (LCP) and light saturation point (LSP), as well as the dark respiration rate ( $R_D$ ). Furthermore, the

mechanistic Farquhar-von Caemmerer-Berry (FvCB) biochemical model, described by Farquhar et al.<sup>[7]</sup>, has been widely used by numerous researchers to estimate key biochemical parameters of carbon assimilation through fitting A/Ci curves<sup>[7-9]</sup>. This model has been widely used to simulate CO<sub>2</sub> assimilation and applied for decades<sup>[7,10]</sup>. It clearly explains the physiological properties of photosynthesis of intact leaves<sup>[5]</sup>, and the parameters reflecting the biochemical properties of leaves as being easier to estimate from this model with gas exchange measurements<sup>[8]</sup>.

The structural organization of plant leaves can either facilitate or constrain the photochemical reactions underlying photosynthesis<sup>[11,12]</sup>. Therefore, the leaf structural changes may affect photosynthetic efficiency<sup>[6,13]</sup>. However, although a variety of ecological studies have revealed a correlation between leaf structural parameters and photosynthetic performance<sup>[14-16]</sup>, there were contradictory differences between foliage structural and functional variables in the previous work<sup>[17]</sup>. Therefore, in order to understand the effect of leaf structure on each of the photosynthetic performance parameters, it is necessary to analyze the relationship between leaf structure and leaf photosynthesis and to comprehensively evaluate the importance of each component in leaf photosynthesis. Furthermore, evaluation of the relationship between leaf structure and leaf photosynthesis could provide ecophysiological evidence for understanding the structural properties of leaves and how they affect photosynthetic performance. Even though a number of studies analyze the effects of leaf structure on photosynthetic performance<sup>[11,14]</sup>, there has been limited synthetic analysis of the correlations between leaf structural

parameters and photosynthetic performance<sup>[12]</sup>. In particular, few studies have been conducted on coffee. Therefore, this study aimed to explore the relationship between leaf structural parameters and photosynthetic performance, and to clarify the importance of these correlations through a comprehensive evaluation. Obtaining these results may provide useful information for future coffee breeding and plantation management.

## Materials and methods

### Study site characterization and plant material

The experiment was conducted in a shade coffee plantation of the Dehong Tropical Agriculture Research Institute of Yunnan (DTARI), Ruili, southwest China.

The study was conducted from 2019 to 2021. The experimental site was situated at latitude 24.025 south and longitude 97.855 west at an altitude of 890 meters above sea level with an average temperature of 22.2 °C and precipitation of 1,260 mm. The soil type in the plantation is acidic lateritic red soil.

The cultivars used for this study was 'Catimor' which is an interspecies hybrid derived from the cross between Caturra (*C. arabica* L.) and Timor (*C. arabica* × *C. canephora* Pierre ex Froehner). The coffee trees were approximately five years old and spaced 1 m × 2 m. Shade trees (*Dimocarpus longan* Lour.) were planted in East to West row orientation at 12 m × 4 m dimension.

Fourteen plants with consistent growth were selected in the coffee plantation. Three leaves were taken from 14 cohort plants in different directions for measurement of leaf gas exchange parameters. Measurements were taken from the third or fourth completely expanded leaf pair at the apex of the plagiotropic (lateral) branches, located in the upper third of the plant.

### Gas exchange measurements

The leaf gas exchange parameters (net CO<sub>2</sub> assimilation rate (A), stomatal conductance to water vapor (g<sub>s</sub>), transpiration rate (E), internal CO<sub>2</sub> concentration (C<sub>i</sub>), vapor pressure deficit (VPD), and leaf water use efficiency (WUE = A·E<sup>-1</sup>) and environmental indicators (leaf temperature (TL), relative humidity (RH) and ambient temperature (TA)) were determined simultaneously by using a portable photosynthesis system CIRAS 3 (PP Systems, USA). Leaf water use efficiency (WUE), representing the units assimilated for CO<sub>2</sub> per unit of water lost through transpiration, was determined *via* the user manual version 1.06. All measurements were taken on sunny days from 09:00 to 11:30 and 15:00 to 18:00. The referenced CO<sub>2</sub> concentration was set at 390 ppm using a buffer bottle, the temperature at 27 °C, flow rate at 300 μmol·s<sup>-1</sup>, relative humidity at 50% ± 10%, and irradiance at 800 μmol·m<sup>-2</sup>·s<sup>-1</sup>. The leaf photosynthetic (LRCs) and internal CO<sub>2</sub> response (A/C<sub>i</sub>) curves were constructed by using leaf gas exchange measurement. To collect data for building LRCs, net photosynthesis was measured at 0, 50, 100, 150, 200, 250, 300, 350, 400, 500, 600, 700, 800, 1,000, and 1,200 μmol·m<sup>-2</sup>·s<sup>-1</sup> (PAR) with a cuvette environment that maintained leaf temperature at 27 °C, reference CO<sub>2</sub> concentration at 400 ppm. The gas exchange rate usually stabilizes within approximately 3–4 min after the leaf tissue is clamped in the leaf chamber. Data for the construction of the A/C<sub>i</sub> curves were collected immediately following the LRC measurements from the same sampled leaf. P<sub>n</sub> was measured at CO<sub>2</sub> concentrations of 400, 300, 200, 100,

150, 250, 350, 450, 550, 650, 750, 850, 950, 1,050, 1,250, 1,450 and 1,650 μmol·m<sup>-2</sup>·s<sup>-1</sup> at photosynthesis saturating irradiance 800 μmol·m<sup>-2</sup>·s<sup>-1</sup>, which light intensity is sufficiently high to saturate the photosynthetic machinery without causing photoinhibition. A total of 41 LRC and 42 A/C<sub>i</sub> curves were generated.

### Measurement of leaf anatomical traits

Following the gas exchange measurement, five samples from leaves of each plant were harvested, sealed in polyethylene bags, and immediately brought back to the laboratory. Two segments (3 mm × 5 mm) were cut from each leaf halfway between the leaf apex and base. The segments were dehydrated in sucrose solutions, followed by the inclusion with Gum Arabic aqueous solution. Transverse sections (7–10 μm) thickness was cut using a rotary microtome (Leica CM3050S, Germany) and stained with toluidine blue. Surface impressions were made manually and stained with 0.1% safranin aqueous solution. For each leaf, five transversal and surface sections were selected systematically to measure the leaf thickness (LT), upper cuticle thickness (UCT), upper epidermal thickness (UET), palisade tissue thickness (PT), spongy tissue thickness (ST), lower epidermal thickness (LET), lower cuticle thickness (LCT), stomatal density (*d*), and guard cell length (*l*) and width (*w*) using a binocular microscope binocular with 10× and 40× objectives (Leica DM5000 B). Subsequently, five micrographs per section were captured with a photomicroscope equipped with a Leica DFC500 camera (Leica Microsystems, Rijswijk, The Netherlands). Images were analyzed using Leica Leica LAS X software. Total stomatal pore area (TSP) was calculated as  $d \times 1/4\pi \times l \times w$ , assuming pore was an ellipse<sup>[15,18,19]</sup>. Here *d* is the stomatal frequency calculated by dividing the stomatal count by *t* field area, *l* is the guard cell length, and *w* is the guard cell width.

### Calculations and statistical analysis

LRCs were fitted by applying a modified rectangular hyperbola model using Photosynthetic Calculation Software 4.1.1<sup>[20–22]</sup>. The modified rectangular hyperbola model is described by Eqn (1).

$$P_n(I) = \alpha \frac{1 - \beta I}{1 + \gamma I} I - R_d \quad (1)$$

where *P<sub>n</sub>* is the net photosynthetic rate (μmol·CO<sub>2</sub>·m<sup>-2</sup>·s<sup>-1</sup>), *I* is the photosynthetic photon flux density (μmol·m<sup>-2</sup>·s<sup>-1</sup>), *I<sub>c</sub>* is compensation irradiance, *β* and *γ* are the coefficients which are independent of *I*, and *α* is the absolute value of slope between *I* = 0 and *I* = *I<sub>c</sub>*.

For *I* = 0, the quantum yield at this point is defined as intrinsic quantum yield (IQY), which is given by Eqn (2).

$$IQY = \alpha(1 + (\gamma + \beta)I_c) \quad (2)$$

The apparent quantum yield (AQY) ignored the Kok effect is obtained by Eqn (3).

$$AQY = \alpha \frac{1 + (\gamma - \beta)I_c - \gamma\beta I_c^2}{(1 + \gamma I_c)^2} \quad (3)$$

For *I* = 0, the rate of dark respiration (*R<sub>d</sub>*) is Eqn (4).

$$R_d = -P_n(I_0) = -\alpha I_c \quad (4)$$

The saturation irradiance *I<sub>sat</sub>* is obtained by Eqn (5).

$$I_{sat} = \frac{\sqrt{(\beta + \gamma)/\beta} - 1}{\gamma} \quad (5)$$

The maximum photosynthetic rate  $P_{nmax}$  is given by Eqn (6).

$$P_{nmax} = \alpha \left( \frac{\sqrt{\beta + \gamma} - \sqrt{\beta}}{\gamma} \right)^2 - R_d \quad (6)$$

A/C<sub>i</sub> curves were fit by uploading the datasets to the website (<http://Leafweb.ornl.gov>) to estimate the parameters ( $R_d$ ,  $V_{cmax}$ ,  $J_{max}$ , TPU,  $I^*$ ,  $g_i$ ). In this study, the A/C<sub>i</sub> curves were taken at the saturation light level. Thus, the rate of electron transport ( $J$ ) was to assume the maximum rate of electron transport ( $J_{max}$ ).

The relationship between photosynthetic capacity and leaf anatomical traits was analyzed by calculating the Pearson correlation coefficient. The correlation coefficients were partitioned into direct and indirect effects using path analysis. The path diagram in Fig. 1 was utilized to examine the causal pathways between nine selected leaf anatomical traits and each photosynthetic parameter. In Fig. 1, the direct effects of leaf anatomical traits on photosynthetic parameters are represented by single-headed arrows, while coefficients of intercorrelations between leaf anatomical traits are represented by double-headed arrows.

Path coefficient analysis was calculated as the method

described by Dewey & Lu<sup>[23]</sup>.

$$r_{ij} = p_{ij} + \sum r_{ik} p_{kj} \quad (7)$$

where  $r_{ij}$  represents the simple correlation coefficient between the independent character (i) and dependent character (j) as measured by the correlation coefficient,  $p_{ij}$  is the component of direct effects of the independent character (i) and dependent character (j) as measured by the path coefficient and,  $\sum r_{ik} p_{kj}$  is the summation of components of the indirect effect of a given independent character (i) on the given dependent character (j) via all other independent characters (k). An uncorrelated residue (U) was estimated using Eqn (8).

$$U = \sqrt{1 - R^2} \quad (8)$$

where  $R^2$  is the coefficient of determination,  $R^2 = \sum r_{ij} p_{ij}$ .

The multiple criteria decision analysis (MCDA) was used to evaluate comprehensive evaluation of the relationship between leaf anatomical traits and photosynthetic parameters. The objective weight of each photosynthetic parameter ( $W_j$ ) is derived by using the Criteria Importance Though Intercrieria Correlation (CRITIC) method, which reflects the relative impor-

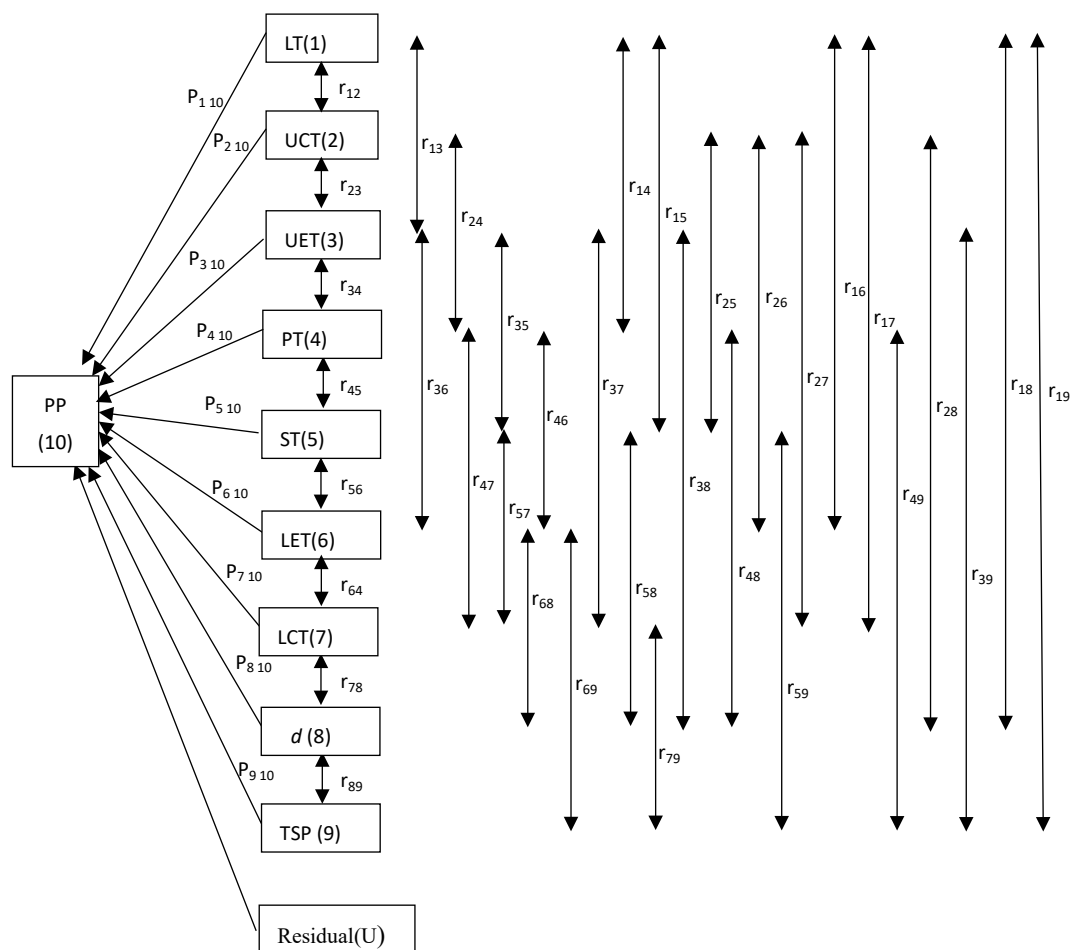


**Fig. 1** Path diagram for the relationship between leaf anatomical traits and photosynthetic parameters. The direct effects ( $P_{ij}$ ) of leaf anatomical traits on the photosynthetic parameter (PP) are represented by single-headed arrows, while the indirect effects ( $r_{ij}P_{ij}$ ) of leaf anatomical traits are shown by double-headed arrows. Subscript designations for leaf anatomical traits and photosynthetic parameters are identified numerically as follows: (1) LT = leaf thickness; (2) UCT = upper cuticle thickness; (3) UET = upper epidermal thickness; (4) PT = palisade tissue thickness; (5) ST = spongy tissue thickness; (6) LET = lower epidermal thickness; (7) LCT = lower cuticle thickness; (9)  $d$  = stomatal density; (10) TSP = total stomatal pore area; and (10) PP = photosynthetic parameters. The photosynthetic parameters (PP) are IQY, AQY,  $\alpha$ ,  $P_{nmax}$ ,  $I_{sat}$ ,  $I_c$ ,  $R_D$ ,  $R_d$ ,  $V_{cmax}$ ,  $J_{max}$ , TPU,  $I^*$ ,  $g_i$ ,  $C_{ir}$ ,  $g_s$ , VPD, A, E, WUE.

tance by applying the comparative and conflict information among the indicators<sup>[24]</sup>. Two calculation steps are used to evaluate the weights of each criterion using the CRITIC method.

Step 1 is to normalize the decision matrix using Eqn (9).

$$\bar{x}_{ij} = \frac{x_{ij} - x_j^{\min}}{x_j^{\max} - x_j^{\min}} \quad (9)$$

Step 2 is to calculate the weights for each criterion

$$C_j = \sigma_j \sum_{j=1}^n (1 - R_{ij}) \quad (10)$$

$$W_j = C_j / \sum_{j=1}^m C_j \quad (11)$$

where,  $\sigma_j$  was the standard deviation of each criterion  $j$ , and  $R_{ij}$  is the linear correlation coefficient between the vectors  $X_i$  and  $X_j$ . The comprehensive evaluation value of the effects of leaf anatomical traits on photosynthetic parameters were estimated from Eqn (12).

$$Q_i = \sum_{j=1}^n (w_j \times D_{ij}) \quad (12)$$

where  $D_{ij}$  was the correlation (direct effects, indirect effects, and Pearson's correlation, respectively) between leaf anatomical trait  $i$  and photosynthetic parameter  $j$ . All statistical analyses were conducted with IBM SPSS Statistics 24.

## Results

The photosynthetic light-response curve (Fig. 2) was well fitted by the modified rectangular hyperbola model ( $R^2 = 0.945 \pm 0.006$ ) described by Ye<sup>[22]</sup>. The  $P_n$  increased with  $I$  below the  $I_{sat}$ . As  $I$  rise above the  $I_{sat}$ ,  $P_n$  decreases as  $I$  increase, implying a photoinhibition phenomenon. The calculated AQY would be  $0.028 \pm 0.003$  if the Kok effect was ignored. This value was lower than  $\alpha$  ( $0.031 \pm 0.003$ ) and the IQY ( $0.033 \pm 0.003$ ). The maximum  $P_n$  values calculated by the modified rectangular hyperbola model at the  $I_{sat}$  of  $621.762 \pm 37.358 \mu\text{mol (photon) m}^{-2}\text{s}^{-1}$  was  $5.131 \pm 0.478 \mu\text{mol (CO}_2\text{) m}^{-2}\text{s}^{-1}$  for coffee leaf. The values of  $I_c$  and  $R_D$  were  $60.238 \pm 11.332 \mu\text{mol (photon) m}^{-2}\text{s}^{-1}$  and  $0.930 \pm 0.098 \mu\text{mol (CO}_2\text{) m}^{-2}\text{s}^{-1}$ , respectively.

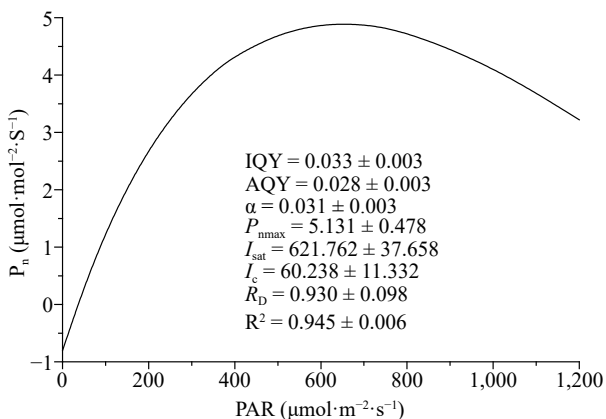


**Fig. 2** Photosynthetic light-response curve of coffee plants. Data shown in the figure indicate mean  $\pm$  standard error. IQY – intrinsic quantum yield; AQY – apparent quantum yield;  $\alpha$  – the absolute value of slope between  $I = 0$  and  $I = I_c$ ;  $P_{nmax}$  – maximum photosynthetic rate [ $\mu\text{mol (CO}_2\text{) m}^{-2}\text{s}^{-1}$ ];  $I_{sat}$  – light saturation point [ $\mu\text{mol (photon) m}^{-2}\text{s}^{-1}$ ];  $I_c$  – light compensation point [ $\mu\text{mol (photon) m}^{-2}\text{s}^{-1}$ ];  $R_D$  – dark respiration [ $\mu\text{mol (CO}_2\text{) m}^{-2}\text{s}^{-1}$ ].

The  $A/C_i$  curve was fitted with the interactive website ([www.leafweb.ornl.gov](http://www.leafweb.ornl.gov)) based on the FvCB model structure<sup>[25]</sup>. Figure 3 shows the response of  $A$  (net photosynthesis) to  $C_i$  for coffee leaves. The fitted parameter values for  $V_{cmax}$ ,  $J_{max}$ ,  $T_p$ ,  $R_d$ ,  $\Gamma^*$ ,  $g_i$ , and  $K_{oc}$  were  $61.749 \pm 5.394$ ,  $63.165 \pm 3.859$ ,  $5.316 \pm 0.576$ ,  $3.225 \pm 0.441$ ,  $3.309 \pm 0.333$ ,  $1.101 \pm 0.287$ ,  $103.096 \pm 11.721$ , respectively. The transition between the Rubisco and RuBP regeneration-limited states ( $C_{i,c}$ ) occurs around 20 Pa of intercellular  $\text{CO}_2$  (Fig. 3).

Cross-sections observed under a light microscope revealed that the coffee leaves were bifacial, with a typical well-differentiated single layer of elongated palisade mesophyll cells on the adaxial side and large spongy mesophyll cells on the abaxial side. The large spongy mesophyll cells at the abaxial side comprised almost 60% of the total blade thickness (Table 1). Of all the tissues, the palisade tissue thickness (PT) showed the highest variation in dimensions ( $CV = 13.243\%$ ). The stomatal density ( $d$ ) and total stomatal pore area (TSP) were 152.028 and 0.439, respectively (Table 1).

Pearson's correlation analysis established correlations between 19 physiological indexes and leaf anatomical traits (Table 2). The UCT showed negative correlation with the indexes of IQY, AQY,  $\alpha$ ,  $I_{sat}$ , and  $g_i$  ( $p < 0.05$ ). The UET was positively related to AQY,  $\alpha$ , and  $P_{max}$  ( $p < 0.05$ ) and negatively related to  $I_c$ ,  $R_d$ ,  $C_i$ , and VPD ( $p < 0.05$ ) (Table 2). The relationship between PT and IQY, AQY, and  $\alpha$  was significantly negative ( $p < 0.05$ ). A significant negative correlation was between LET and  $I_c$  ( $p < 0.05$ ). The Pearson correlation coefficient between LCT and  $I_{sat}$  was significantly negative ( $p < 0.05$ ). The guard cell width ( $w$ ) significantly affected  $I_c$  and  $R_d$  ( $p < 0.05$ ). The guard cell length ( $l$ ) was negatively correlated with IQY, AQY,  $\alpha$ , and  $I_{sat}$  and positively correlated to  $J_{max}$  ( $p < 0.05$ ). A strong positive ( $p < 0.01$ ) correlation was found between stomatal density ( $d$ ) and  $J_{max}$ . However, the LT and ST did not

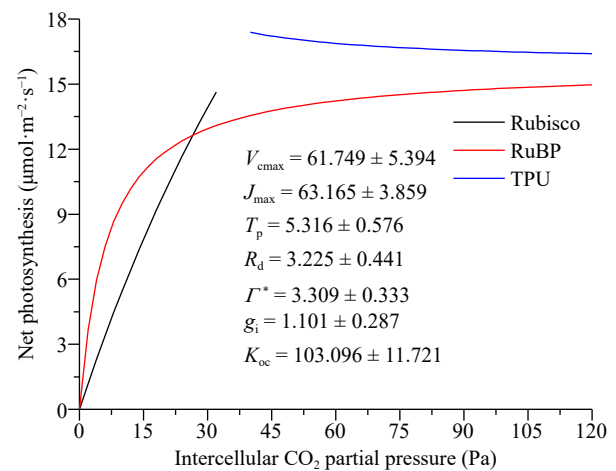


**Fig. 3** The  $A/C_i$  curves for the coffee plants. Data shown in the figure indicate mean  $\pm$  stand error.  $C_i$  – Intercellular  $\text{CO}_2$  concentration ( $\mu\text{mol}\cdot\text{mol}^{-1}$ );  $V_{cmax}$  – Maximal Rubisco carboxylation rate ( $\mu\text{mol}\cdot\text{m}^{-2}\cdot\text{s}^{-1}$ );  $J_{max}$  – Maximal electron transport rate ( $\mu\text{mol}\cdot\text{m}^{-2}\cdot\text{s}^{-1}$ );  $T_p$  – Rate of triose phosphate export from the chloroplast ( $\mu\text{mol}\cdot\text{m}^{-2}\cdot\text{s}^{-1}$ );  $R_d$  – Day respiration ( $\mu\text{mol}\cdot\text{m}^{-2}\cdot\text{s}^{-1}$ );  $\Gamma^*$  –  $\text{CO}_2$  compensation point in the absence of dark respiration (Pa);  $g_i$  – Internal (mesophyll) conductance to  $\text{CO}_2$  transport ( $\mu\text{mol}\cdot\text{m}^{-2}\cdot\text{s}^{-1}\cdot\text{Pa}^{-1}$ );  $K_{oc}$  – A composite parameter (Pa):  $K_{oc} = K_c(1 + O/K_o)$ .

Leaf anatomical traits influence on photosynthesis in Arabica coffee

**Table 1.** The components of anatomical tissues in Arabica coffee leaf.

Leaf anatomy		Mean	SE	CV (%)	Proportion of leaf thickness (%)
Tissue components (μm)	LT	255.627	1.832	4.645	100.000
	UCT	5.497	0.042	4.962	2.154
	UET	23.681	0.291	7.957	9.279
	PT	51.014	1.042	13.243	19.913
	ST	153.285	1.245	5.264	59.969
	LET	17.908	0.195	7.056	7.023
Stomatal characteristics	LCT	4.243	0.040	6.121	1.662
	<i>w</i> (μm)	8.252	0.048	3.733	
	<i>l</i> (μm)	27.874	0.208	4.839	
	<i>d</i> (No./mm <sup>2</sup> )	152.028	1.942	8.277	
	TSP	0.439	0.006	8.886	

LT – leaf thickness, UCT – upper cuticle thickness, UET – upper epidermal thickness, PT – palisade tissue thickness, ST – spongy tissue thickness, LET – lower epidermal thickness, LCT – lower cuticle thickness, *w* – guard cell width, *l* – guard cell length, *d* – stomatal density, TSP – total stomach pore area.

significantly affect photosynthetic efficiency according to the Pearson correlation study.

Path analysis was performed to reveal the direct and indirect effects of leaf anatomy traits on photosynthetic capacity. The results indicating the effect are shown in Fig. 4 & Supplemental Table S1. Although correlation analysis suggested no significant correlations between LT and photosynthetic capacity variables ( $p > 0.05$ ), LT had relatively high direct positive effects on  $g_i$  (0.545), IQY (0.467),  $R_d$  (0.476), and  $\alpha$  (0.420) and a high negative direct effect on  $I_{sat}$  (–0.415) (Fig. 4a). The path coefficient analysis revealed that UCT had a high magnitude negative direct effect on IQY (–0.686),  $\alpha$  (–0.676), AQY (–0.652),  $g_s$  (–0.685), and TPU (–0.517). The UET had highly negative direct effects on  $R_d$  (–0.859) and TPU (–0.632), but moderate positive direct effects on E (0.479),  $P_{max}$  (0.437), and A (0.423). The PT exhibited an impressive negative direct effect on TPU (–0.474),

AQY(–0.514),  $\alpha$  (–0.506), and IQY (–0.487), while a high positive direct effect was shown between PT and E (0.445). The ST had a high positive direct effect on  $I_{sat}$  (0.630) and WUE (0.583), and a similar high negative direct effect on VPD (–0.579). LET had high positive direct effects on WUE (0.482),  $g_i$  (0.416), TPU (0.462), and  $V_{cmax}$  (0.398), a relatively high negative direct effect LET and  $I_c$  (–0.314) and VPD (–0.311). The LCT showed a negative direct effects  $V_{cmax}$  (–0.539),  $I_c$  (–0.370),  $R_D$  (–0.411),  $J_{max}$  (–0.378),  $g_i$  (–0.340) and VPD (–0.328), but a moderate positive direct effect on  $I^*$  (0.359). The stomatal density (*d*) exhibited large positive direct effects on  $P_{max}$  (0.672)  $I_{sat}$  (0.893), WUE (0.673), and  $J_{max}$  (0.482), and high negative direct effects on  $C_i$  (–0.772) and VPD (–0.576) were found. The negative direct effect of TSP on  $I_{sat}$  (–1.05) was very high, followed by  $P_{max}$  (–0.519) and WUE (–0.496). In addition, TSP showed high positive direct effects on  $g_i$  (0.613) and VPD (0.579).

The estimates of the indirect effect of leaf anatomical trait on photosynthetic capacity via other leaf anatomical traits were presented in Fig. 4b and Supplemental Table S2. According to this figure, the LT had highly negative indirect effects on IQY (–0.511),  $\alpha$  (–0.453), AQY (–0.403),  $R_d$  (–0.369), and  $g_i$  (–0.338), but a high positive indirect effect on  $I_{sat}$  (0.358). The UCT had high indirect effect on  $I_{sat}$  (–0.479),  $I_c$  (–0.477),  $J_{max}$  (–0.423), TPU (0.372), IQY (0.350), AQY (0.330), and  $\alpha$  (0.344). The UET indirectly exerted relatively high positive effects on TPU (0.424) and  $R_d$  (0.382). Similarly, the PT exhibited relatively high positive indirect effects on  $R_d$  (0.508) and TPU (0.486). The ST had high negative on  $I_{sat}$  (–0.441),  $I^*$  (–0.389), and WUE (–0.399), but relatively high positive indirect effects on  $g_i$  (0.318) and E (0.374). The LET revealed a positive indirect effect on  $R_D$  (–0.338),  $V_{cmax}$  (–0.379), TPU (–0.469),  $g_i$  (–0.487) through other anatomical traits. The LCT had negative indirect effects on IQY (–0.386), AQY (–0.497),  $\alpha$  (–0.454), and  $I_{sat}$  (–0.642), but a highly positive indirect effects LCT on VPD (0.433) and  $V_{cmax}$  (0.377). Stomatal characteristics (*d*) play a key role in determining photosynthesis. In this study, the stomatal density (*d*) indirectly

**Table 2.** The correlation between leaf anatomical traits and photosynthetic parameters.

Parameters	LT	UCT	UET	PT	ST	LET	LCT	<i>w</i>	<i>l</i>	<i>d</i>	TSP
IQY	–0.044 ns	–0.336*	0.296 ns	–0.343*	–0.010 ns	0.000 ns	–0.232 ns	0.175 ns	–0.315*	0.232 ns	0.103 ns
AQY	–0.024 ns	–0.322*	0.386*	–0.394*	0.012 ns	0.039 ns	–0.224 ns	0.197 ns	–0.358*	0.206 ns	0.068 ns
$\alpha$	–0.033 ns	–0.332*	0.351*	–0.375*	0.005 ns	0.022 ns	–0.230 ns	0.189 ns	–0.342*	0.217 ns	0.082 ns
$P_{max}$	0.178 ns	–0.108 ns	0.324*	–0.036 ns	0.103 ns	0.100 ns	–0.065 ns	–0.037 ns	–0.233 ns	0.143 ns	–0.003 ns
$I_{sat}$	–0.057 ns	–0.359*	0.157 ns	–0.278 ns	0.189 ns	–0.202 ns	–0.377*	–0.227 ns	–0.460**	0.031 ns	–0.313*
$I_c$	–0.064 ns	–0.143 ns	–0.324*	0.164 ns	–0.008 ns	–0.336*	–0.174 ns	–0.323*	–0.071	0.017 ns	–0.150 ns
$R_D$	0.025 ns	–0.234 ns	–0.195 ns	0.204 ns	0.057 ns	–0.190 ns	–0.150 ns	–0.243 ns	–0.005 ns	0.156 ns	0.036 ns
$R_d$	0.097 ns	0.161 ns	–0.477**	0.101 ns	0.003 ns	–0.129 ns	0.071 ns	–0.354*	0.133 ns	–0.043 ns	–0.114 ns
$V_{cmax}$	–0.021 ns	–0.097 ns	0.009 ns	0.106 ns	0.188 ns	0.019 ns	–0.161 ns	0.172 ns	–0.003 ns	0.139 ns	0.200 ns
$J_{max}$	–0.086 ns	–0.169 ns	–0.104 ns	–0.047 ns	–0.035 ns	–0.188 ns	–0.183 ns	–0.003 ns	–0.212 ns	0.403**	0.246 ns
TPU	–0.033 ns	–0.145 ns	–0.209 ns	0.012 ns	0.045 ns	–0.008 ns	0.015 ns	–0.162 ns	0.045 ns	0.245 ns	0.183 ns
$I^*$	–0.210 ns	0.181 ns	–0.086 ns	–0.159 ns	–0.239 ns	0.228 ns	0.119 ns	–0.163 ns	0.104 ns	–0.285 ns	–0.276 ns
$g_i$	0.207 ns	–0.433*	0.311 ns	–0.092 ns	0.371 ns	–0.071 ns	–0.420*	–0.006 ns	–0.301 ns	–0.149 ns	–0.301 ns
$C_i$	–0.066 ns	0.108 ns	–0.396**	0.257 ns	–0.125 ns	–0.164 ns	0.187 ns	–0.053 ns	0.311*	–0.080 ns	0.077 ns
$g_s$	0.140 ns	–0.111 ns	0.278 ns	0.073 ns	0.044 ns	0.146 ns	0.053 ns	0.005 ns	–0.085 ns	0.174 ns	0.116 ns
VPD	–0.023 ns	0.071 ns	–0.372*	0.281 ns	–0.143 ns	–0.230 ns	0.106 ns	–0.063 ns	0.221 ns	0.052 ns	0.148 ns
A	0.157 ns	–0.079 ns	0.346*	0.007 ns	0.049 ns	0.203 ns	0.047 ns	0.048 ns	–0.117 ns	0.149 ns	0.094 ns
E	0.196 ns	–0.057 ns	0.224 ns	0.191 ns	0.031 ns	0.068 ns	0.106 ns	0.002 ns	0.003 ns	0.164 ns	0.158 ns
WUE	0.049 ns	–0.115 ns	0.350*	–0.230 ns	0.184 ns	0.226 ns	–0.142 ns	0.041 ns	–0.216 ns	0.074 ns	–0.038 ns

LT – leaf thickness, UCT – upper cuticle thickness, UET – upper epidermal thickness, PT – palisade tissue thickness, ST – spongy tissue thickness, LET – lower epidermal thickness, LCT – lower cuticle thickness, *w* – guard cell width, *l* – guard cell length, *d* – stomatal density, TSP – total stomach pore area. Ns = non-significant. \*, \*\* represent significant; highly significant differences at 5% and 1% probability levels, respectively.

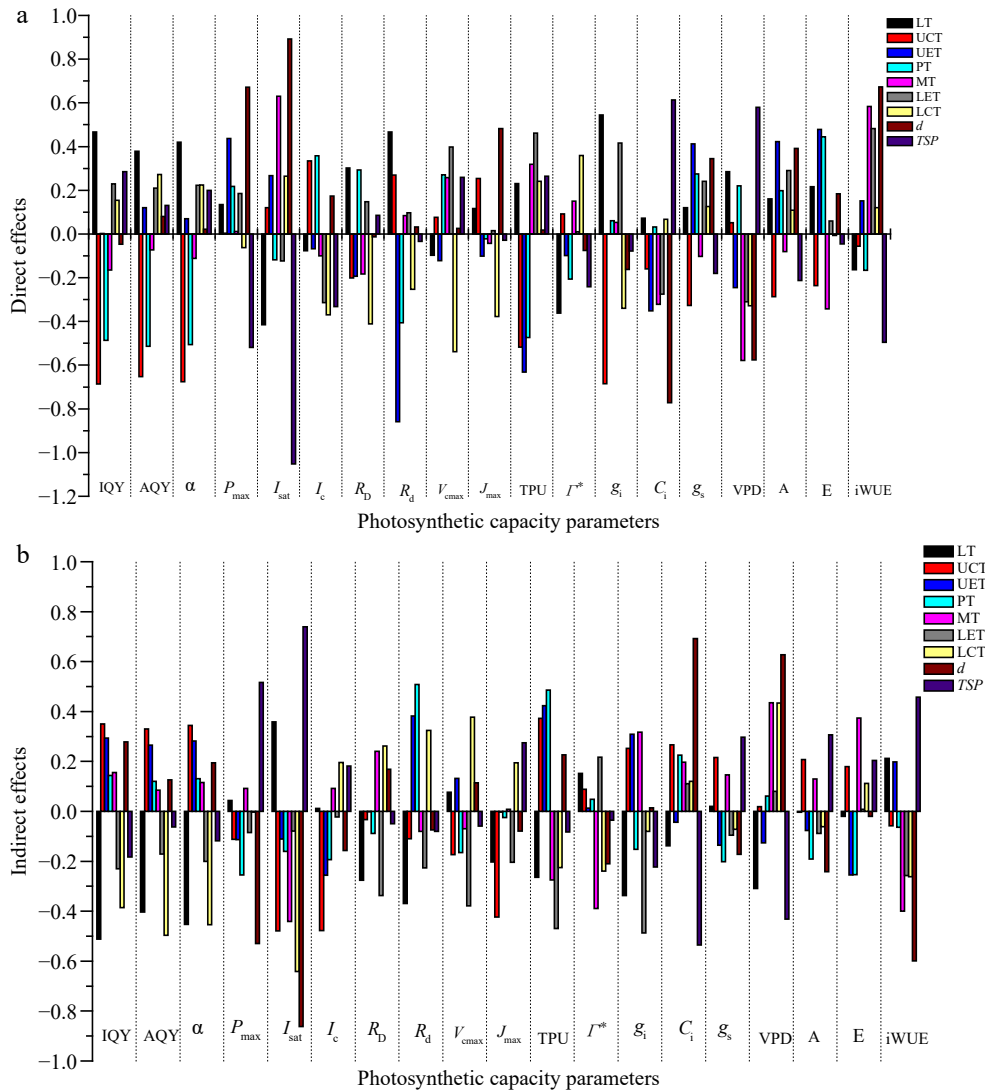


**Fig. 4** (a) Direct and (b) indirect effects of each leaf anatomical traits through other traits on photosynthetic parameters. LT – leaf thickness, UCT – upper cuticle thickness, UET – upper epidermal thickness, PT – palisade tissue thickness, ST – spongy tissue thickness, LET – lower epidermal thickness, LCT – lower cuticle thickness,  $w$  – guard cell width,  $l$  – guard cell length,  $d$  – stomatal density, TSP – total stomach pore area. The residual effect of IQY, AQY,  $\alpha$ ,  $P_{max}$ ,  $I_{sat}$ ,  $I_c$ ,  $R_D$ ,  $R_d$ ,  $V_{cmax}$ ,  $J_{max}$ , TPU,  $I^*$ ,  $g_i$ ,  $C_i$ ,  $g_s$ , VPD, A, E, and WUE was 0.799, 0.760, 0.775, 0.849, 0.737, 0.859, 0.908, 0.755, 0.883, 0.887, 0.860, 0.877, 0.644, 0.817, 0.858, 0.821, 0.840, 0.858, and 0.801, respectively.

influenced  $P_{max}$ ,  $I_{sat}$  and WUE with a relatively high negative magnitudes ( $-0.529$ ,  $-0.862$ , and  $-0.599$ ), but had a relatively high positive indirect effect of stomatal density ( $d$ ) on  $C_i$  (0.692), and VPD (0.628). The TSP presented a relatively high negative indirect effect on  $C_i$  ( $-0.536$ ) and VPD ( $-0.432$ ), but highly positive indirect effect of TSP on  $I_{sat}$  (0.739),  $P_{max}$  (0.516), and WUE (0.458).

To identify the combined effect of leaf anatomical traits on photosynthetic parameters, a comprehensive evaluation analysis was conducted. Based on the evaluation values ( $Q_i$ ), the ranking of the comprehensive scores of relationships between photosynthetic capacity and leaf anatomical traits was shown in Table 3. For the direct effect, the LT had the highest comprehensive score, followed by LET,  $d$ , ST, PT, UET, TSP LCT, and UCT. For the comprehensive score of indirect effect of leaf anatomical traits on photosynthetic capacity, the UET held the highest comprehensive score, and UCT was the second, followed by ST, TSP, PT,  $d$ , LCT, LT, and LET. Similar results from the Pearson

correlation analyses of comprehensive assessments revealed that the first comprehensive assessment score was  $d$  and that the second assessment score was also ST. Then, the ranking order after the third was UET, LT, TSP, PT, LET, LCT, and UCT.

## Discussion

Several studies involving gas exchange measurements of coffee leaves have been performed. These studies indicate that the photosynthetic capacity of coffee leaves varies with varying environmental conditions<sup>[26–29]</sup>. For single coffee leaves, the saturating irradiance is between 300 and 700  $\mu\text{mol}\cdot\text{m}^{-2}\cdot\text{s}^{-1}$ , with shade leaves showing a lower value than lower sun leaves<sup>[27]</sup>. This study found that the saturating irradiance of sun leaves was about 620  $\mu\text{mol photons m}^{-2}\cdot\text{s}^{-1}$ , which was consistent with the result of the above mention. Quantum yields revealed the relationship between a given light-dependent product and the number of absorbed photons<sup>[30]</sup>. Quantum

**Table 3.** Comprehensive ordering of the effects of leaf anatomical traits on photosynthetic capacity using the CRITIC method.

Anatomical traits	Direct effects		Indirect effects		Pearson's correlation	
	Comprehensive score	Ranking	Comprehensive score	Ranking	Comprehensive score	Ranking
LT	0.160	1	-0.127	8	0.033	4
UCT	-0.175	9	0.055	2	-0.121	9
UET	-0.025	6	0.063	1	0.038	3
PT	-0.010	5	-0.003	5	-0.013	6
ST	-0.009	4	0.052	3	0.043	2
LET	0.132	2	-0.151	9	-0.020	7
LCT	-0.048	8	-0.029	7	-0.077	8
<i>d</i>	0.095	3	-0.024	6	0.072	1
TSP	-0.043	7	0.041	4	-0.002	5

LT – leaf thickness, UCT – upper cuticle thickness, UET – upper epidermal thickness, PT – palisade tissue thickness, ST – spongy tissue thickness, LET – lower epidermal thickness, LCT – lower cuticle thickness, *w* – guard cell width, *l* – guard cell length, *d* – stomatal density, TSP – total stomatal pore area.

yield is 0 when none of the light energy is used in photosynthesis. Quantum yield is 1 when all the absorbed light is used. Based on the results of Ye, the quantum yield decreased with *l* increasing<sup>[22]</sup>. Thus, the IQY was higher than AQY. In the past, there were several pertinent points about the maximal photosynthetic rates of coffee leaves. For example, Kumar & Tieszen and Cannell have pointed out that the maximal photosynthetic rates of sun leaves of coffee are around 7  $\mu\text{mol CO}_2 \text{ m}^{-2}\text{s}^{-1}$  and 8.8  $\mu\text{mol CO}_2 \text{ m}^{-2}\text{s}^{-1}$ , respectively<sup>[26,31]</sup>. However, Bote et al. reported that the maximal photosynthetic rates of sun leaves of coffee were lower than 7  $\mu\text{mol CO}_2 \text{ m}^{-2}\text{s}^{-1}$  with a larger N supply<sup>[32]</sup>. In this study, the maximal photosynthetic rates were lower than the observations of Kumar & Tieszen and Cannell and consistent with the results of Bote et al.<sup>[26, 31, 32]</sup>. For coffee leaves, light saturation would lead to an excess of electron transport capacity<sup>[33]</sup>. Therefore, a higher  $J_{\text{max}}$  was observed under light saturation. In addition, the values of  $V_{\text{cmax}}$  and  $J_{\text{max}}$  were larger than the results reported by Martins et al.<sup>[33]</sup>.

The correlation analysis is a great utility method for understanding the relationships between variables. In this study, significant correlations between photosynthetic capacity and leaf anatomical traits were observed, indicating that leaf anatomical traits could affect photosynthetic capacity. Despite the correlation coefficients could provide a good way to understand the relationships between variables, the cause and effect relationships between variables could not be estimated<sup>[34]</sup>. Path analysis, a method that investigates the causal relationship, gives detailed understanding of positive and negative correlations between traits<sup>[34]</sup>. The result of the path analysis is shown in Fig. 3, indicating that there were high-level direct and indirect effects of leaf anatomical traits on photosynthetic capacity. This may explain the importance of leaf structure in photosynthesis. However, the estimated residual effect in this study was high (0.661-0.908), indicating that additional characters which affect photosynthetic capacity are not included in the investigation. For leaf photosynthesis, the overall photosynthetic limitation can be partitioned into different components, such as stomatal, mesophyll, and biochemical limitations<sup>[35]</sup>. The stomatal and mesophyll limitations in coffee leaves accounted for 0.30 and 0.38, respectively<sup>[33]</sup>. This is consistent with the results, where about 30% of the variability in photosynthetic capacity was contributed by the characters studied in the path analysis in this study. In order to quantitatively evaluate the effect of each structure of the leaf on photosynthesis, the comprehensive evaluation values calculated by using Equa-

tion (13) introduced in the methods. The ordering Pearson's correlation of comprehensive score showed that stomatal density (*d*) and spongy tissue thickness (ST) were the most important leaf anatomical traits for coffee leaf photosynthesis. For Arabica coffee, leaf photosynthesis is greatly limited by  $\text{CO}_2$  diffusion<sup>[36]</sup>. The  $\text{CO}_2$  diffusion from the air to the leaf mesophyll is mainly modulated by the stomatal conductance ( $g_s$ ), which is associated with stomatal density (*d*)<sup>[5,37]</sup>. According to the comprehensive score of indirect effect, the stomatal density (*d*) also had the highest comprehensive score. This indicates that stomatal density (*d*) is essential for coffee leaf photosynthesis. In fact, higher stomatal density will increase  $g_s$  by increasing the same total pore area<sup>[37]</sup> and allow more  $\text{CO}_2$  diffusion. This may partly explain why the total stomatal pore area (TSP) had higher comprehensive evaluation values in the effect of coffee leaf photosynthesis. Therefore, the result of a comprehensive evaluation revealed that Arabica coffee leaf of stomatal characteristics, such as guard cell width and length, stomatal density, and stomatal pore surface, plays a significant role in leaf photosynthetic capacity. This finding was also consistent with previous work, indicating that stomatal characteristics of the leaf are closely associated with photosynthesis by controlling the water loss and  $\text{CO}_2$  uptake<sup>[38,39]</sup>.

The leaf thickness was strongly positively correlated with the fraction of intercellular air space in the leaves<sup>[17]</sup>. The result obtained in this study showed that leaf thickness (LT) affects photosynthesis mainly through direct and indirect effects, given that the  $\text{CO}_2$  diffusion in the gaseous phase is about three orders of magnitude larger than in the liquid<sup>[11]</sup>. Thus, the diffusive resistance should not necessarily increase considerably with increasing leaf thickness<sup>[40]</sup>. The result of direct effects of leaf thickness (LT) on photosynthetic capacity confirmed that increasing leaf thickness may increase  $g_i$ . Moreover, due to the chloroplasts adhering to the inner surface of exposed mesophyll cell walls, thicker leaves provide space for more chloroplasts per unit leaf area<sup>[5]</sup> and possess more chloroplast surface area, which results in a substantial increase in carbon dioxide absorption because of a larger surface area for diffusion<sup>[40]</sup>. The direct effects of the path analysis indicate that greater leaf thickness would facilitate  $\text{CO}_2$  diffusion in the mesophyll ( $g_i$ ). Furthermore, thicker leaves may have higher total contents of Rubisco and leaf N per unit area<sup>[41]</sup>, so it advantageous to realize high photosynthetic rates in highlight environments<sup>[42]</sup>. In this study, leaf thickness (LT) affects photosynthetic indexes that were IQY,  $\alpha$ , AQY,  $R_{\text{dr}}$ ,  $g_{\text{ir}}$  and  $l_{\text{sat}}$  and, consequently, photo-

synthesis rate. Therefore, the result of a comprehensive evaluation revealed that leaf thickness (LT) was the most important role in the direct effect on leaf photosynthetic capacity.

The structure of the leaf cuticle consists of epicuticular wax, birefringent wax embedded in cutin, cutin matrix, and pectic substance<sup>[43]</sup>. The epicuticular wax can decrease light by scattering<sup>[32]</sup>. Similar results have been found in this study where an increase in upper cuticle thickness (UCT) could result in a decrease in IQY, AQY, and  $\alpha$ , which were related to light absorption in photosynthesis. The most cutin matrix in the cuticle is heterogeneous, and the areas of embedded waxes exhibit birefringence in polarized light<sup>[43]</sup>. This heterogeneous structure of the leaf cuticle may affect epidermal focusing, allowing actinic light to penetrate deeper into the mesophyll<sup>[32]</sup>. These findings most likely explained the significant relationship between cuticle thickness and quantum yield of photosynthesis, such as IQY, AQY, and  $\alpha$ . In addition, the cuticle thickness would increase resistance to CO<sub>2</sub> diffusion<sup>[44]</sup>, and the negative relationships between UCT and LCT and photosynthetic parameters were also observed in this study.

The epidermal cell usually has a large transparent central vacuole and lacks mature chloroplasts, thus the light can directly pass from these cells into the mesophyll<sup>[32]</sup>. However, these epidermal cells have various shapes, such as planoconvex, spherical, conical, or some other convex shape<sup>[45]</sup>. The curved outermost epidermal cell wall can affect the focal point within the leaf<sup>[46]</sup>. However, the result of Brodersen & Vogelmann showed that there was no relation between the convexity of epidermal cells and the absorbance of diffuse light<sup>[47]</sup>. Although two contradictory hypotheses have been proposed concerning the impacts of epidermal cells on photosynthesis, the significant relationship between UET and photosynthetic capacity parameters in this study examined epidermal lens effects on many photosynthetic parameters and elucidated epidermal cells property plays an important role in photosynthetic capacity.

The columnar palisade tissue minimizes light scattering when the incident light collimated with the columnar palisade<sup>[48]</sup>. As a result, palisade tissue allows large amounts of light to penetrate the chloroplasts within the leaf<sup>[48]</sup>. The present study has revealed a remarkable relation between quantum yields and PT. However, the results of this study indicated that PT increase would directly decrease the IQY, AQY, and  $J_{max}$ . This circumstance is very difficult to comprehend. Generally, palisade tissue has much more chloroplasts compared with other leaf tissue<sup>[49]</sup>. Thus, the photosynthetic activity of the palisade tissue would be higher. Indeed, the shape of cells in the leaves is strongly associated with photosynthetic performance by affecting the movement and distribution of chloroplasts<sup>[50]</sup>. There was a great variety of dimensions of the palisade tissue thickness (PT) in this study. Coordinated regulation of leaf cell shape and chloroplast motion according to light conditions is essential for efficient leaf photosynthesis<sup>[50]</sup>. This work could partially explain the result of a negative direct effect of PT on photosynthetic parameters.

The concentration of CO<sub>2</sub> in the mesophyll is affected by air temperature, and each degree rise in temperature above 24 °C results in a 20 ppm rise in CO<sub>2</sub> concentration<sup>[51]</sup>. However, Khairi & Hall's studies of citrus photosynthesis revealed that mesophyll conductance to CO<sub>2</sub> decreased as temperature

increased from 22 °C to around 40 °C<sup>[52]</sup>. In the analysis of the effects of leaf anatomical traits on photosynthetic capacity, the spongy tissue thickness (ST) had larger indirect effects and Pearson's correlation comprehensive score, suggesting that spongy tissue thickness (ST) plays an important role in the photosynthetic process. Furthermore, Martins et al. demonstrated that mesophyll thickness is related to water flux and gas exchange per leaf area<sup>[33]</sup>, which is consistent with the findings of this study. The spongy tissue thickness (ST) had direct effects on WUE and VPD. On the other hand, the irregularly shaped spongy cells alternating with air spaces increase light absorption due to the increased optical path length through a leaf<sup>[11]</sup>, and this absorbed light will be advanced for photosynthesis<sup>[31,47]</sup>. Therefore, the high direct spongy tissue thickness (ST) effects upon  $I_{sat}$  were also observed in this study. In fact, the increase in spongy tissue thickness (ST) would increase the surface area of chloroplasts exposed to intercellular airspace, which was associated with CO<sub>2</sub> transfer conductance<sup>[53]</sup>. Although there was little relationship between spongy tissue thickness (ST) and photosynthetic parameters, high direct spongy tissue thickness (ST) effects upon  $I_{sat}$ , WUE, and VPD were observed.

Stomatal density (SD) is a factor associated with the photosynthetic rates of the leaf<sup>[54]</sup>. The CO<sub>2</sub> diffusion conductance is influenced by the density and arrangement of the stomata<sup>[11]</sup>. For the coffee leaf, the net carbon assimilation rate (A) is greatly governed by the diffusive conductance of CO<sub>2</sub>, thus the photosynthesis of the coffee leaf was largely limited by a diffusive factor<sup>[55]</sup>. Stomata have traditionally been thought to play an important role in controlling CO<sub>2</sub> diffusion<sup>[55]</sup> and were a key parameter in *C. arabica* photosynthesis<sup>[29]</sup>. Among the various stomatal characters, stomatal density plays a major role in gas exchange and photosynthesis<sup>[56]</sup>. In this study, it is shown that stomatal density had the highest comprehensive scores compared with other anatomical traits on indirect effects and Pearson's correlation comprehensive evaluation. In addition, structural modification of the stomata is one of the key factors affecting stomatal conductance<sup>[30]</sup>. The result of this study also showed that the guard cell length ( $l$ ) significantly correlated positively with  $C_i$ .

For light absorption, although the result of Martins et al. showed that the guard cell length did not change in response to light treatments<sup>[33]</sup>, there was a significant correlation with IQY and AQY. The coordination between increased initiation of stomata cells and expansion of epidermal cells was observed in coffee leaves, implying that there was an optimization of the trade-off between transpiration costs and CO<sub>2</sub> assimilation<sup>[33]</sup>. In addition, the size and density of the stomata largely affect the diffusive conductance of the leaves to CO<sub>2</sub>, and the balance between the amount of CO<sub>2</sub> required for photosynthesis and the level of water availability is also determined by the stomatal traits<sup>[37]</sup>. Thus, lower epidermal stomatal density had a significant correlation with photosynthetic parameters or direct effects and indirect effects on photosynthetic parameters. Moreover, these traits also had larger comprehensive scores in a comprehensive evaluation, which means that stomatal density was a key parameter in the regulation of photosynthesis of *C. arabica*.

## Conclusions



Many leaf anatomical traits significantly affect photosynthetic parameters. This result provided holistic relationships between leaf anatomical traits and photosynthetic parameters in coffee. It is tempting to suggest that these relationships might, to some extent, explain the photosynthetic behavior of coffee (*C. arabica* L.). The relationships between leaf anatomical traits and photosynthetic parameters emphasize the importance of leaf anatomy in determining photosynthesis at the tissue level. Moreover, these correlations between leaf anatomical traits and photosynthetic parameters were useful to explore the impact of different anatomical features on photosynthetic efficiency and accordingly provide some information to design leaf anatomy for enhanced photosynthetic efficiency. To a certain extent, path analysis and comprehensive evaluation could indicate an interrelationship between photosynthetic capacity and leaf anatomical traits. However, the causal interrelationship between photosynthetic parameters and leaf anatomical traits is less clear. In addition, this study only analyzed the effect of anatomical structure on photosynthesis for one Catimor type of Arabica coffee. Effects on photosynthesis are typically genotype dependent, with some varieties being more tolerant to partial shading than others. Future studies should compare different Arabica coffee varieties for their anatomical traits and photosynthetic response to suitability in agroforestry-based production systems. Despite this, the result of the study also suggests that thinner leaves and higher stomatal densities might support a higher photosynthetic capacity. This result may be useful information for coffee breeding programs and plantation management.

## Author contributions

The authors confirm contribution to the paper as follows: conceptualization and research design: Xiao Z, Ma G; project administration: Bai X, Li J; investigation and fieldwork: Zhao M, Su L; data analysis & manuscript preparation: Xiao Z; resources: Zhou H. All the authors read and edited the manuscript, and approved the final version.

## Data availability

The datasets generated and analyzed during the current study are available from the corresponding author on reasonable request.

## Acknowledgments

This research was funded by the Coffee Industry Technology Delegation of Zhenkang County, Yunnan Province (202204BI090009), Basic Research Project of the Dehong Tropical Agriculture Research Institute of Yunnan (DTARI-JJ2020-02), and the Yunnan Dehong Integrated Experiment Station of the National Cassava Industry Technology System, Coffee Cloud Platform (CARS-11-YNLJH).

## Conflict of interest

The authors declare that they have no conflict of interest.

**Supplementary Information** accompanies this paper at (<https://www.maxapress.com/article/doi/10.48130/bpr-0023-0035>)

## Dates

Received 15 September 2023; Revised 8 October 2023; Accepted 26 October 2023; Published online 2 January 2024

## References

1. Franck N, Vaast P. 2009. Limitation of coffee leaf photosynthesis by stomatal conductance and light availability under different shade levels. *Trees* 23:761–69
2. Beer JW, Muschler RG, Somarriba E, Kass D. 1997. Shade management in coffee and cacao plantations. *Agroforestry Systems* 38:139–64
3. International Coffee Council (ICO). 2015. Coffee in China. *International Coffee Council, 115<sup>th</sup> Session, 28 Sept. – 2 Oct. 2015, Milan, Italy*. Milan, Italy: International Coffee Organization. [www.ico.org/documents/cy2014-15/icc-115-7e-study-china.pdf](http://www.ico.org/documents/cy2014-15/icc-115-7e-study-china.pdf)
4. Ma GR, Liu HQ, Tian SM, Bai XH, Zhao MZ, et al. 2019. Soil nutrient status in coffee plantation of Yunnan and the main factors related to quality of green coffee beans. *Journal of Plant Nutrition and Fertilizers* 25(7):1222–29
5. Lambers H, Oliveira RS. 2019. Photosynthesis, respiration, and long-distance transport: Photosynthesis. In *Plant Physiological Ecology*. Switzerland: Springer. pp. 11–114. [https://doi.org/10.1007/978-3-030-29639-1\\_2](https://doi.org/10.1007/978-3-030-29639-1_2)
6. Herrmann HA, Schwartz JM, Johnson GN. 2020. From empirical to theoretical models of light response curves - linking photosynthetic and metabolic acclimation. *Photosynthesis Research* 145:5–14
7. Farquhar GD, von Caemmerer S, Berry JA. 1980. A biochemical model of photosynthetic CO<sub>2</sub> assimilation in leaves of C<sub>3</sub> species. *Planta* 149:78–90
8. Wang Q, Chun AJ, Fleisher D, Reddy V, Timlin D, et al. 2017. Parameter estimation of the Farquhar — von Caemmerer — Berry biochemical model from photosynthetic carbon dioxide response curves. *Sustainability* 9:1288
9. Sun Y, Gu L, Dickinson RE, Pallardy SG, Baker J, et al. 2014. Asymmetrical effects of mesophyll conductance on fundamental photosynthetic parameters and their relationships estimated from leaf gas exchange measurements. *Plant, Cell & Environment* 37:978–94
10. GU L, Pallardy SG, Tu K, Law BE, Wullschlegel SD. 2010. Reliable estimation of biochemical parameters from C<sub>3</sub> leaf photosynthesis-intercellular carbon dioxide response curves. *Plant, Cell & Environment* 33:1852–74
11. Oguchi R, Onoda Y, Terashima I, Tholen D. 2018. Leaf anatomy and function. In *The leaf: a platform for performing photosynthesis*, ed. Adams III W, Terashima I. Switzerland: Springer Cham. pp. 97–139. [https://doi.org/10.1007/978-3-319-93594-2\\_5](https://doi.org/10.1007/978-3-319-93594-2_5)
12. Tholen D, Boom C, Zhu XG. 2012. Opinion: prospects for improving photosynthesis by altering leaf anatomy. *Plant Science* 197:92–101
13. Akhka A, Reid I, Clarke DD, Dominy P. 2001. Photosynthetic light response curves determined with the leaf oxygen electrode: minimisation of errors and significance of the convexity term. *Planta* 214:135–41
14. Bolhàr-Nordenkampf HR, Draxler G. 1993. Functional leaf anatomy. In *Photosynthesis and production in a changing environment*, eds. Hall DO, Scurlock JMO, Bolhàr-Nordenkampf HR, Leegood RC, Long SP. Netherlands: Springer Dordrecht. pp. 91–112. [https://doi.org/10.1007/978-94-011-1566-7\\_7](https://doi.org/10.1007/978-94-011-1566-7_7)
15. James SA, Bell DT. 2001. Leaf morphological and anatomical characteristics of heteroblastic *Eucalyptus globulus* ssp. *globulus* (Myrtaceae). *Australian Journal of Botany* 49:259–69
16. Vogelman TC, Nishio JN, Smith WK. 1996. Leaves and light capture: light propagation and gradients of carbon fixation within leaves. *Trends in Plant Science* 1:65–70
17. Niinemets Ü. 1999. Components of leaf dry mass per area – thickness and density – alter leaf photosynthetic capacity in reverse directions in woody plants. *New Phytologist* 144:35–47

18. Battie-Laclau P, Laclau JP, Beri C, Mietton L, Muniz MRA, et al. 2014. Photosynthetic and anatomical responses of *Eucalyptus grandis* leaves to potassium and sodium supply in a field experiment. *Plant, Cell & Environment* 37:70–81
19. Batos B, Vilotić D, Orlović S, Miljković D. 2010. Inter and intra-population variation of leaf stomatal traits of quercus robur I In northern serbia. *Archives of Biological Sciences* 2010,62(4):1125–36
20. Ye ZP, Yu Q. 2008. Comparison of new and several classical models of photosynthesis in response to irradiance. *Journal of Plant Ecology (Chinese Version)* 32(6):1356–61
21. Ye ZP. 2010. A review on modeling of responses of photosynthesis to light and CO<sub>2</sub>. *Chinese Journal of Plant Ecology* 34:727–40
22. Ye ZP. 2007. A new model for relationship between irradiance and the rate of photosynthesis in *Oryza sativa*. *Photosynthetica* 45:637–40
23. Dewey DR, Lu KH. 1959. A correlation and path-coefficient analysis of components of crested wheatgrass seed production 1. *Agronomy Journal* 51:515–18
24. Diakoulaki D, Mavrotas G, Papayannakis L. 1995. Determining objective weights in multiple criteria problems: The critic method. *Computers & Operations Research* 22:763–70
25. Gu L, Sun Y. 2014. Artefactual responses of mesophyll conductance to CO<sub>2</sub> and irradiance estimated with the variable *J* and online isotope discrimination methods. *Plant Cell & Environment* 37:1231–49
26. Kumar D, Tieszen LL. 1980. Photosynthesis in *Coffea arabica* I. Effects of light and temperature. *Experimental Agriculture* 16:13–19
27. DaMatta FM. 2004. Ecophysiological constraints on the production of shaded and unshaded coffee: a review. *Field Crops Research* 86:99–114
28. DaMatta FM, Ramalho JDC. 2006. Impacts of drought and temperature stress on coffee physiology and production: a review. *Brazilian Journal of Plant Physiology* 18:55–81
29. Ayalew B. 2018. Impact of shade on morpho-physiological characteristics of coffee plants, their pests and diseases: A review. *African Journal of Agricultural Research* 13:2016–24
30. Taiz L, Zeige E. 2006. Photosynthesis: Physiological and ecological considerations. In *Plant Physiology*. Sunderland Massachusetts: Sinauer Associates, Inc. pp. 179–80.
31. Cannell MGR. 1985. Physiology of the coffee crop. In *Coffee*, eds. Clifford MN, Willson KC. Boston, MA: Springer. pp. 108–34. [https://doi.org/10.1007/978-1-4615-6657-1\\_5](https://doi.org/10.1007/978-1-4615-6657-1_5)
32. Bote AD, Zana Z, Ocho FL, Vos J. 2018. Analysis of coffee (*Coffea arabica* L.) performance in relation to radiation level and rate of nitrogen supply II. Uptake and distribution of nitrogen, leaf photosynthesis and first bean yields. *European Journal of Agronomy* 92:107–14
33. Martins SCV, Galmés J, Cavatte PC, Pereira LF, Ventrella MC, et al. 2014. Understanding the low photosynthetic rates of sun and shade coffee leaves: bridging the gap on the relative roles of hydraulic, diffusive and biochemical constraints to photosynthesis. *PLoS ONE* 9:e95571
34. De Oliveira TB, Peixoto LA, Teodoro PE, De Alvarenga AA, Bhering LL, et al. 2018. Relationship between biochemical and photosynthetic traits with Asian soybean rust. *Annals of the Brazilian Academy of Sciences* 90:3925–40
35. Grassi G, Magnani F. 2005. Stomatal, mesophyll conductance and biochemical limitations to photosynthesis as affected by drought and leaf ontogeny in ash and oak trees. *Plant, Cell & Environment* 28:834–49
36. DaMatta FM, Ronchi CP, Maestri M, Barros RS. 2007. Ecophysiology of coffee growth and production. *Brazilian Journal of Plant Physiology* 19:485–510
37. Rodrigues WP, Silva JR, Ferreira LS, Machado Filho JA, Figueiredo FA, et al. 2018. Stomatal and photochemical limitations of photosynthesis in coffee (*Coffea* spp.) plants subjected to elevated temperatures. *Crop and Pasture Science* 69:317–25
38. Yin Q, Tian T, Kou M, Liu P, Wang L, et al. 2020. The relationships between photosynthesis and stomatal traits on the Loess Plateau. *Global Ecology and Conservation* 23:e01146
39. Sakoda K, Yamori W, Shimada T, Sugano SS, Hara-Nishimura I, et al. 2020. Higher stomatal density improves photosynthetic induction and biomass production in Arabidopsis under fluctuating light. *Frontiers in Plant Science* 11:589603
40. Smith WK, Vogelmann TC, DeLucia EH, Bell DT, Shepherd KA. 1997. Leaf form and photosynthesis. *BioScience* 47:785–93
41. Niinemets Ü, Sack L. 2006. Structural determinants of leaf light-harvesting capacity and photosynthetic potentials. In *Progress in Botany*, eds. Esser K, Lüttge U, Beyschlag W, Murata J. vol. 67 Berlin, Heidelberg: Springer. pp. 385–419. [https://doi.org/10.1007/3-540-27998-9\\_17](https://doi.org/10.1007/3-540-27998-9_17)
42. Terashima I, Hanba YT, Tholen D, Niinemets Ü. 2011. Leaf functional anatomy in relation to photosynthesis. *Plant Physiology* 155:108–16
43. Lee DW, Graham R. 1986. Leaf optical properties of rainforest sun and extreme shade plants. *American Journal of Botany* 73:1100–8
44. Miranda V, Baker NR, Long SP. 1981. Anatomical variation along the length of the *Zea mays* leaf in relation to photosynthesis. *New Phytologist* 88:595–605
45. Jackson D, Skillman J, Vandermeer J. 2012. Indirect biological control of the coffee leaf rust, *Hemileia vastatrix*, by the entomogenous fungus *Lecanicillium lecanii* in a complex coffee agroecosystem. *Biological Control* 61:89–97
46. Vogelmann TC, Bornman JF, Yates DJ. 1996. Focusing of light by leaf epidermal cells. *Physiologia Plantarum* 98:43–56
47. Brodersen CR, Vogelmann TC. 2007. Do epidermal lens cells facilitate the absorption of diffuse light? *American Journal of Botany* 94:1061–66
48. Vogelmann TC, Martin G. 1993. The functional significance of palisade tissue: penetration of directional versus diffuse light. *Plant, Cell & Environment* 16:65–72
49. Terashima I, Inoue Y. 1985. Palisade tissue chloroplasts and spongy tissue chloroplasts in spinach: biochemical and ultrastructural differences. *Plant and Cell Physiology* 26:63–75
50. Gotoh E, Suetsugu N, Higa T, Matsushita T, Tsukaya H, Wada M. 2018. Palisade cell shape affects the light-induced chloroplast movements and leaf photosynthesis. *Scientific Reports* 8:1472
51. Nunes M, Bierhuizen J, Ploegman C. 1968. Studies on productivity of coffee: I. Effect of light, temperature and CO<sub>2</sub> concentration on photosynthesis of *Coffea arabica*. *Acta botanica neerlandica* 17:93–102
52. Khairi MMA, Hall AE. 1976. Comparative Studies of Net Photosynthesis and Transpiration of Some Citrus Species and Relatives. *Physiologia plantarum* 36:35–39
53. Evans JR, Caemmerer SV, Setchell BA, Hudson GS. 1994. The relationship between CO<sub>2</sub> transfer conductance and leaf anatomy in transgenic tobacco with a reduced content of Rubisco. *Functional Plant Biology* 21:475–95
54. Bondada BR, Oosterhuis DM, Wullschlegel SD, Kim KS, Harris WM. 1994. Anatomical considerations related to photosynthesis in cotton (*Gossypium hirsutum* L.) leaves, bracts, and the capsule wall. *Journal of Experimental Botany* 45:111–18
55. Araujo WL, Dias PC, Moraes GABK, Celin EF, Cunha RL, et al. 2008. Limitations to photosynthesis in coffee leaves from different canopy positions. *Plant Physiology and Biochemistry* 46:884–90
56. Pompelli MF, Martins SCV, Celin EF, Ventrella MC, Damatta FM. 2010. What is the influence of ordinary epidermal cells and stomata on the leaf plasticity of coffee plants grown under full-sun and shady conditions? *Brazilian Journal of Biology* 70:1083–88



Copyright: © 2024 by the author(s). Published by Maximum Academic Press, Fayetteville, GA. This article is an open access article distributed under Creative Commons Attribution License (CC BY 4.0), visit <https://creativecommons.org/licenses/by/4.0/>.